JOURNAL OF SPACECRAFT AND ROCKETS
Vol. 32, No. 1, January–February 1995

Subsonic Drag Reduction of the Space Shuttle Orbiter

Mohammad Javed Khan,* Anwar Ahmed,† and Edmundo Varela-Rodriguez*
Texas A&M University, College Station, Texas 77843

Various near-wake flow-modifying devices were experimentally evaluated for their effectiveness in increasing base pressure of the Space Shuttle Orbiter at low subsonic speed. The results confirmed the strong three-dimensional character of the Orbiter near wake. A base cavity was found to be the most effective mechanism for increasing base pressure. However, for this mechanism to be effective, the cavity had to be longer than the main engine nozzles. Surface characteristics of the base cavity exposed to freestream had a strong influence on the base pressure. The trapped-vortex mechanism due to a back step was found to be effective in increasing the base pressure only in the region of the orbital-maneuvering-system pods. A combination of base-cavity and trapped-vortex mechanisms increased the base pressure by 25%, and the reduction in total drag was approximately 6%.

Nomenclature

A	= base area
AOA	= angle of attack
C_d	= total-drag coefficient
C_{pb}	= base-pressure coefficient
d	= depth of groove
L/D	= lift-to-drag ratio
OMS	= orbital maneuvering system
P	= static pressure
q	= dynamic pressure ($0.5\rho V^2$)
V	= velocity
α	= angle of groove
ΔC_d	= change in total drag coefficient, $(C_{d\,\text{baseline}} - C_d)/C_{d\,\text{baseline}}$
ΔC_p	= change in base-pressure coefficient $(C_{pb} - C_{pb\,\text{baseline}})/C_{pb\,\text{baseline}}$
ρ	= density of air

Subscripts

b	= base
baseline	= without flow modification devices
∞	= freestream conditions

Introduction

ALTHOUGH the design of the Space Shuttle Orbiter is based on extensive wind-tunnel tests and analyses, the approach and landing tests (ALT) of the Orbiter confirmed that the conceived prototype under the design and mission constraints had a steep glide slope, high landing speeds, and a high sink rate. These characteristics are a result of low L/D ratio and translate into a smaller margin at touchdown. The landing performance of the Orbiter would therefore be improved by increasing the L/D ratio. Lift characteristics of the Orbiter can be enhanced by various methods, e.g., the application of vortex generators, foreplane vortex-induced lift, or redesign of the wing; however, this would mean building an entirely new aerodynamic configuration. Another approach would be to consider methods of reducing the drag of the Orbiter. Approximately 63% of its total drag consists of base-pressure drag.[1] This ratio of base drag to total drag is very large in comparison with conventional aircraft of comparable size but with streamlined aft bodies. Reduction of this large base drag therefore offers possibilities for improving the landing qualities of the Orbiter without a major redesign of aerodynamic configuration.

The base-pressure drag, which is defined as

$$C_{dp} = \int (P_b - P_\infty)\, dA/q_\infty$$

can be decreased by increasing the base pressure P_b. This can be achieved by modification of the near wake. Effectiveness of passive devices, especially splitter plates and various forms of base cavities, for modifying the near wake and thereby reducing the base drag at subsonic, transonic, and supersonic speeds has been reported by various authors for two-dimensional and axisymmetric bodies. Roshko[2] used splitter plates to influence the shedding frequency of a cylinder and also its drag. This phenomenon is primarily attributed to the trapped-vortex concept (Fig. 1a). It has also been exploited for axisymmetric bodies by "stepping" the base[3] and by using base-mounted disks.[4] Various theories have been put forward to explain the base-cavity effect. Nash[5] proposed that disruption/weakening of the vortex shedding was the mechanism responsible for base-drag reduction for two-dimensional bodies. Compton,[6] however, attributed the increase in base pressure to "coflow" (Fig. 1b), in which inhibition of mixing was implicitly assumed as the prime mechanism. Tanner[7] showed the effect of trailing-edge geometry on drag for a blunt-trailing-edge wing. He also reported influence of angle of attack on the effectiveness of a base cavity.[8] Morel[9] carried out a parametric study of the influence of cavity depths on base-drag reduction, concluding that a depth-to-base diameter ratio of 0.2 was most effective in reducing drag. Friedberg and Ahmed[10] investigated the effect of cavity surface grooves on the base pressure of a noncircular cross section. They attribute this influence to alignment of spanwise vorticity in the flow to the streamwise direction which narrows the wake (Fig. 1c). Other authors[11,12] have also investigated these concepts at transonic and supersonic Mach numbers.

Exploration of such devices therefore offered an attractive approach to reducing the excessive base drag of the Orbiter. It should be noted that the base of the Orbiter is three-dimensional and its configuration does not allow the creation of a base cavity in the classical sense (i.e., completely enclosed). In addition, the aft fuselage flares out rather than being boat-tailed, further accentuating the wake.

The objective of this study was to evaluate the effectiveness of various passive devices in modifying the near-wake flow of the Space Shuttle Orbiter to reduce its base-pressure drag. A number of such devices were installed on the Orbiter and tested for their influence on its aerodynamic characteristics. In this paper, however, only the effects of these devices on base pressures and total drag are addressed. Specifically, only those configurations are discussed that resulted in reduction in the base-pressure drag as well as the total drag of the Orbiter. Complete details of all the configurations tested and their aerodynamic effects can be found elsewhere.[13]

Received Oct. 28, 1991; revision received May 14, 1993; accepted for publication May 27, 1993.

*Graduate Student, Department of Aerospace Engineering. Student Member AIAA.

†Assistant Professor, Department of Aerospace Engineering. Member AIAA.

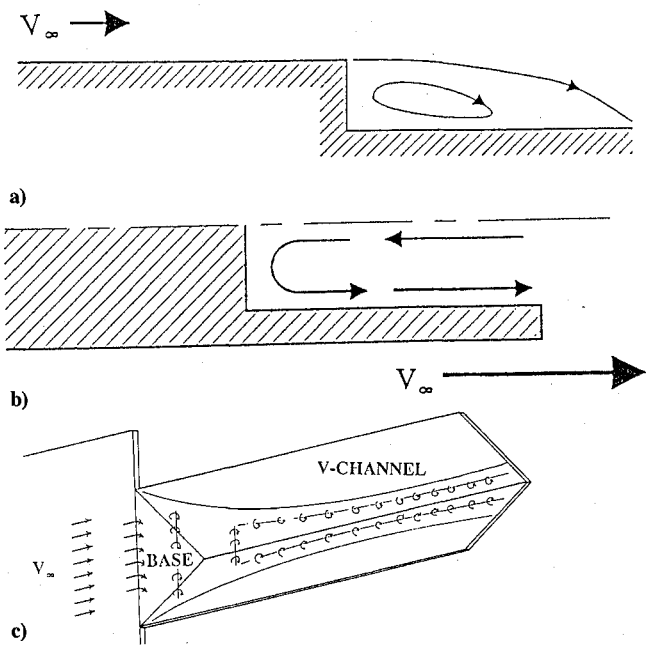

Fig. 1 Generic wake-modification concepts.

Description of Test Facilities and Models

Test Facilities

All experiments were conducted in the 0.61 × 0.91-m (2 × 3-ft) water tunnel and the 2.1 × 3-m (7 × 10-ft) low-speed wind tunnel of the Texas A&M University. The water tunnel, which is a free-surface closed-circuit tunnel, has a maximum speed of 0.76 m/s with a turbulence level of 0.5% of freestream. The tunnel is equipped with a pressurized six-color dye injection system having precision micrometer-controlled flow valves. The model mounting consists of a sting mechanism with continuous control in two axes. The low-speed wind tunnel is a closed-circuit, closed-test-section, low-speed tunnel with a maximum dynamic pressure of 4.788×10^3 kN/m^2. It is equipped with a six-component external balance and an automated data acquisition and processing system for forces/moments as well as pressures.

Orbiter Models

The Orbiter model used for preliminary studies in the water tunnel was a 1:72 scaled plastic model with metallic reinforcement crossplates. One of these plates, extending from the wing tip, was used for mounting the model in the water tunnel. Fifteen dye ports in the model were connected to metallic tubing terminating outside the model for connection with the dye injection system. A 4.05% scale model of wood and metal construction with a removable base plate was used for wind-tunnel tests. The base plate was equipped with 28 pressure ports (Fig. 2) to measure the base pressures. It was designed to facilitate mounting of various side plates used to form the base cavity without interfering with the pressure ports. Tests were conducted with main-engine nozzles mounted on the base plate. The model was mounted on the wind tunnel balance with a three-point support system.

Base Cavities

Side plates extending the fuselage were used to form the base cavity. Two lengths of the plates (10, 20 cm) were tested. These plates could be mounted either flush to create a cavity or offset closer to the fuselage centerline to create a back step. These plates had two types of surfaces: smooth and V-grooved. Two different depths of grooves ($d = 7.5$ and 15 mm), aligned with the freestream and having $\alpha = 60$ deg, were machined in the plates, resulting in a fine and a coarse pitch, respectively. Figure 3a shows a cross section of the plate with grooves. A flush mounted V-grooved plate is shown in Fig. 3b. Plates with porosity were also tested. Porosity is normally defined as the ratio of the surface area of removed material to the total surface area of the cavity. In the present study, as the base configuration was not a completely enclosed cavity (viz., the upper and lower sides were open), such a quantification was not considered useful. The installation of porous plates with a smooth surface forming a backstep is shown in Fig. 4.

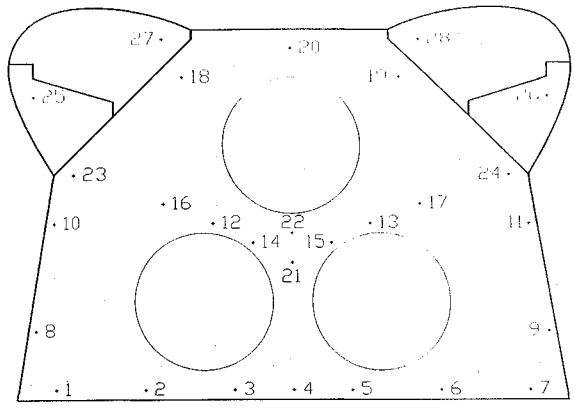

Fig. 2 Location of pressure ports on base plate.

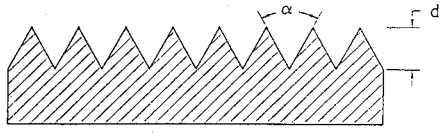

Fig. 3a V-groove geometry.

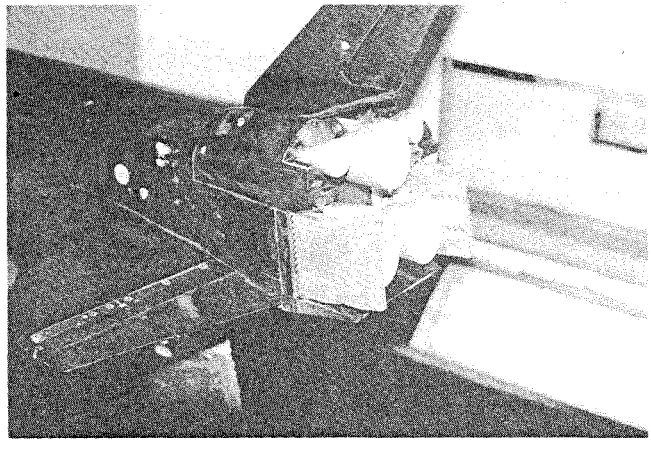

Fig. 3b V-grooved side plates mounted to form a cavity.

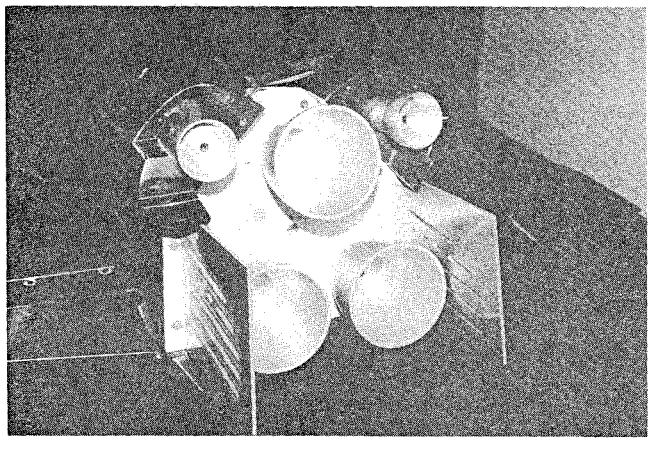

Fig. 4 Smooth side plates mounted to form a back step.

OMS Pod Fairing Plate

This fairing has been used in earlier tests[1] also. It covers the OMS engines' nozzles, forming a back step. Figure 5a is a schematic of the fairing. Its installation on the Orbiter is shown in Fig. 5b.

Various combinations of these devices were also studied.

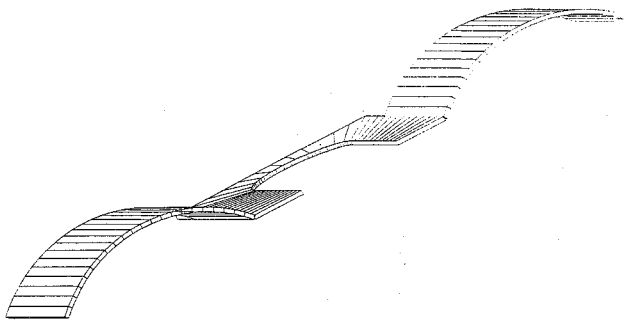

Fig. 5a OMS pod fairing plate.

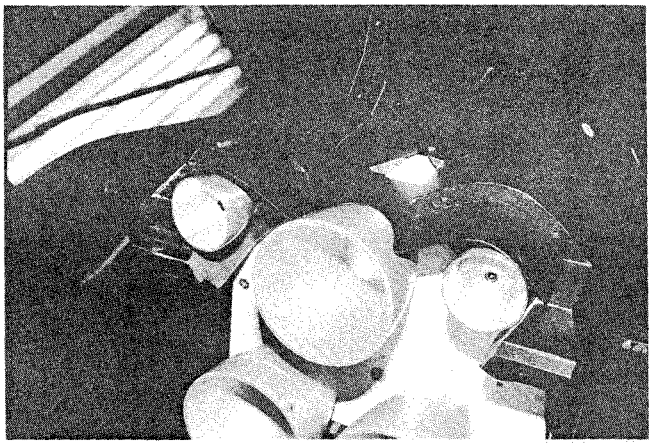

Fig. 5b OMS pod fairing plate installed to form a back step.

Test Plan

The present series of tests consisted of the following:

1) Visualization of the flowfield over the Orbiter and in the near wake, using the water-tunnel facility.
2) Surface-flow visualization in the wind tunnel.
3) Base-pressure measurements in the wind tunnel.
4) Force and moment measurements in the wind tunnel.

Flowfield visualizations in the water tunnel were conducted at a tunnel velocity of 15 cm/s and a Reynolds number of 1.5×10^4. Wind-tunnel tests were conducted at a tunnel dynamic pressure of 4.2×10^3 kN/m^2, which translated to a velocity of 80 m/s and a Reynolds number of 2.6×10^6 based on body length. An angle-of-attack schedule of 0, 5, 10, 15, and 18 deg was followed. The base pressure was determined by averaging the pressure measurements at the 28 ports on the base plate. Forces and moments were measured using the external balance of the wind tunnel.

Results and Discussion

Flow Visualization

Dye injection studies in the water tunnel showed a strong horseshoe vortex at the junction of the OMS pods and body of the Orbiter (Fig. 6a). This vortex was also observed to be influencing the flow over the wing upper surface and was found to be causing large separation in the aft portion of the Orbiter wing-body juncture. The outward flow from this region was significantly influencing the flow separation on the wing. Additionally, a large zone of recirculating flow was observed in the base region. Wind-tunnel surface flow visualization was performed using a light oil-based fluorescent dye. The surface flow patterns, illuminated by ultraviolet light, confirmed the existence of the pod-body juncture vortex (Fig. 6b). Similar flow patterns can also be observed in the flow visualization photographs of Ref. 14.

Effect of Base Cavity

An earlier study[1] reported detrimental effects of base-cavity configurations on the overall drag of the Orbiter. However, the tests in Ref. 1 were carried out for only one cavity length. Dependence of the effectiveness of the base cavity on the base pressure has been well documented in the literature.[6] Tests were therefore conducted on a short as well as a long base cavity. A short base cavity resulted in a very small decrease (approximately 1%) in the total drag, as compared with about 3.5% decrease for a long cavity (Fig. 7) at 0 AOA. This is most probably because the main-engine nozzles do not allow the short plates to develop a base-cavity effect. This trend was observed regardless of the type of surface of the side plates, confirming the dominant influence of the length of the base cavity on the base pressure.

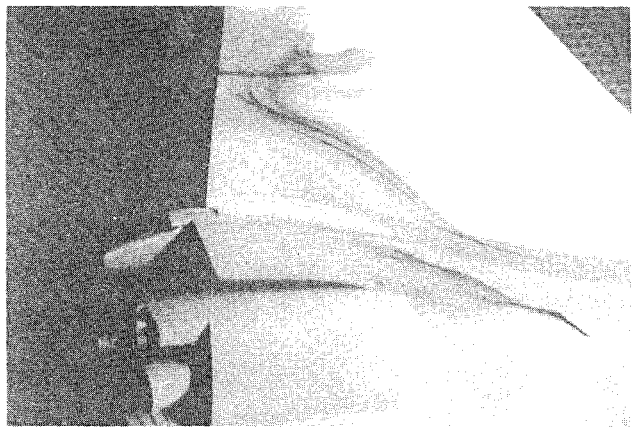

Fig. 6a Water-tunnel flow visualization.

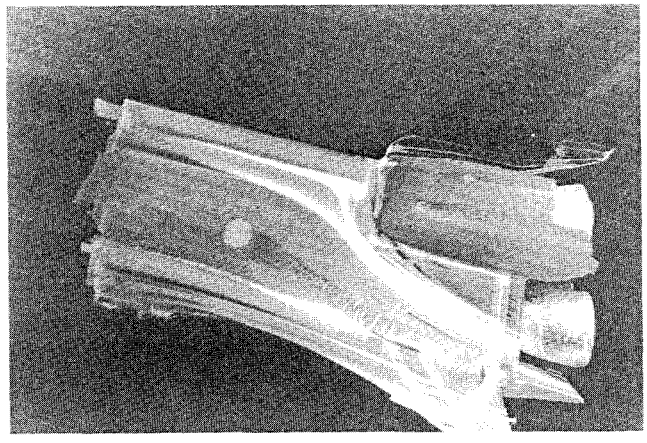

Fig. 6b Wind-tunnel flow visualization.

Surface geometry was also found to be influencing the effectiveness of the plates as a cavity. The V-grooved plates having shorter pitch and smaller depth (V-groove II) were found to be the most effective (Fig. 8) for the entire range of angles of attack. At an AOA of 0 a 19% increase in base pressure was measured, as compared with 13% increase for the smooth plates. The plate with larger pitch and deeper V-grooves (V-groove I) resulted in similar improvements to those with the smooth flat plates.

The increase in base pressure due to porosity in the cavity-producing plates was not appreciable (Fig. 8). This observation is in contrast to earlier work[9] on completely enclosed base cavities. Porosity also resulted in a lower reduction in total drag than for the nonporous cavity.

The OMS pod fairing plate, when installed, formed a back step and was found to increase the base pressure effectively (Fig. 9), despite its being shorter than the short cavity plates. The wake-influencing mechanism was therefore not a base-cavity effect but rather a trapped-vortex effect. The increase in base pressure, however, was less than with the V-grooved and smooth-surface cavities. On the contrary, when the cavity plates were offset closer to the base centerline to introduce a back step, the increase in base pressure was less than 5% (Fig. 9). This indicated that the idea of producing a trapped vortex with a back step and splitter plate was not effective in this part of the base flow. Offsetting the cavity plates also inhibited them from effectively generating the base-cavity effect. These

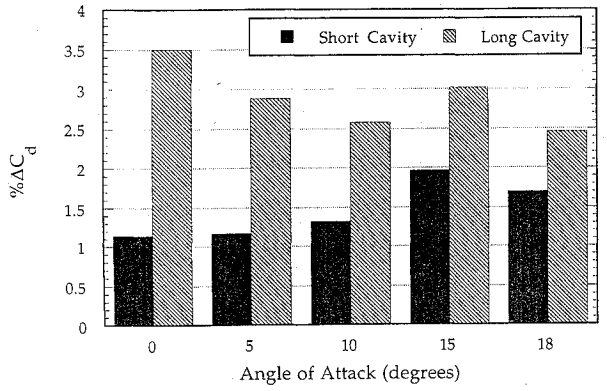

Fig. 7 Effect of base-cavity length on total drag.

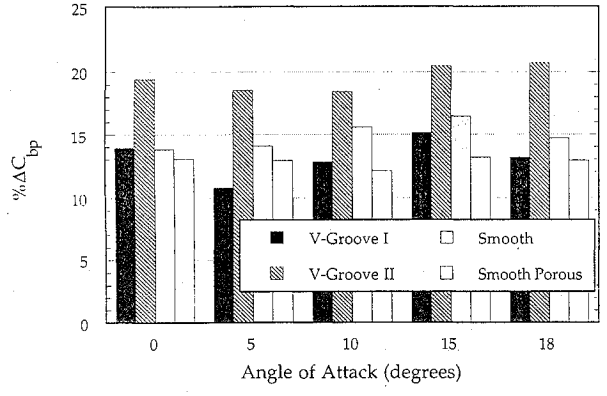

Fig. 8 Effect of base-cavity surface and porosity on base pressure.

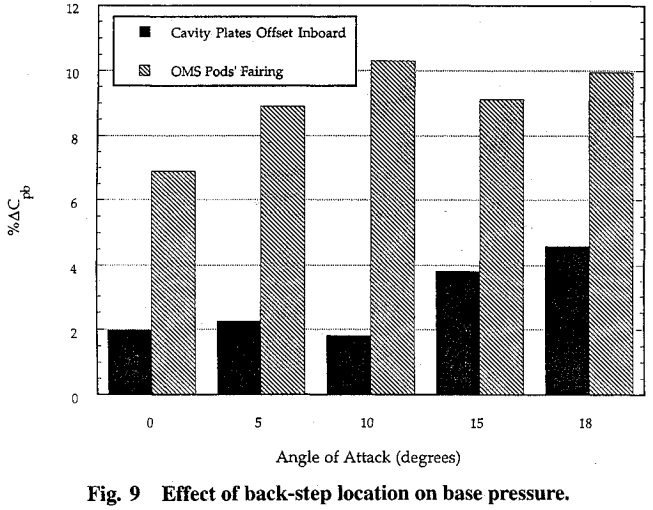

Fig. 9 Effect of back-step location on base pressure.

observations point to the peculiar three-dimensional aerodynamic characteristics of the Orbiter's wake.

Combinations of the base-cavity plates and the OMS pod fairing plate further increased the base pressures. The effect of the combination was found to be linearly additive (Fig. 10).

The total-drag measurements on the Orbiter with the flow-modifying devices installed provided a realistic indication of the effectiveness of the devices by taking into account their contribution to skin friction. It was observed that with increasing angle of attack, the configuration with the OMS pod fairing plate showed a continuous degradation in its effectiveness in reducing total drag and became totally ineffective at an angle of attack of 18 deg (Fig. 11). This was in contrast to the response of the base pressure to this configuration, which was almost independent of the angle of attack. This behavior of the total drag is most probably due to an increased region of attached flow on the main-engine nozzles at higher angles of attack, increasing the skin friction. The base-cavity configurations

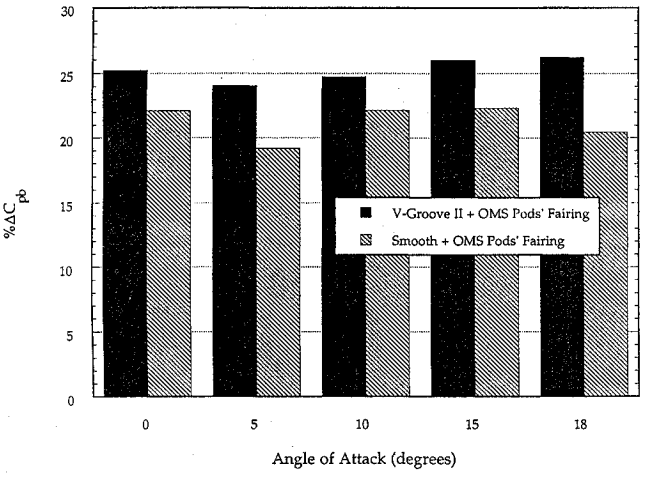

Fig. 10 Effect of various combinations on base pressure.

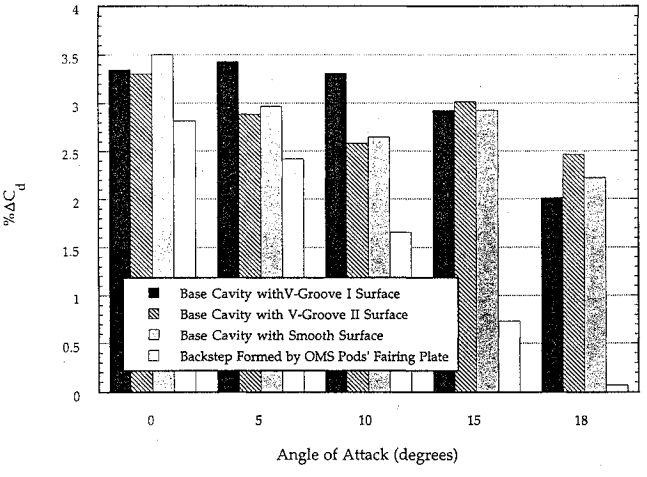

Fig. 11 Effect of various configurations on total drag.

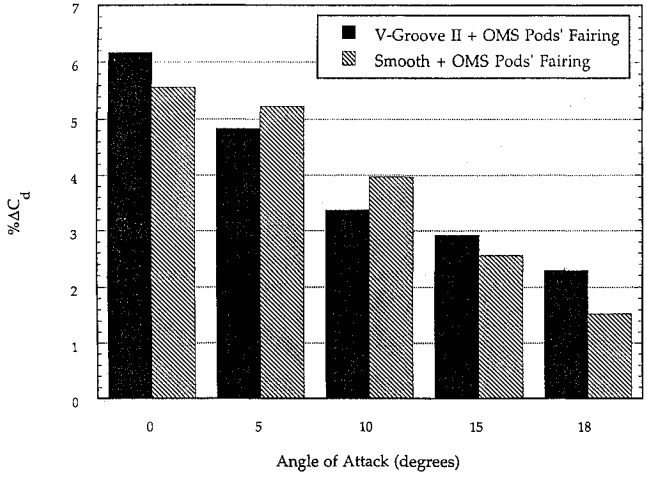

Fig. 12 Effect of various combinations on total drag.

exhibited a much shallower trend in reduction of their effectiveness with increasing angles of attack. The reduction in total drag due to the smooth-surface base cavity was comparable to that due to the grooved-surface base cavity; this was in contrast to their effectiveness as base-pressure-enhancing devices. The V-grooved surface, because of having a larger wetted area, had a higher skin friction, thereby countering the beneficial influence of higher base pressure. Combination of the base-cavity effect and the back-step effect due to OMS pod fairing resulted in further reduction of the total drag (Fig. 12), which was a consequence of the addition of base-pressure increases on combining these devices.

Conclusions

1) The present tests indicate that the juncture vortex due to OMS pods has a strong influence on the flow in the base region of the Orbiter.

2) Base pressures can be effectively reduced by the use of the base-cavity mechanism even though the base may not be fully enclosed to form a cavity in the classical sense.

3) The presence of the main-engine nozzles influences the depth of the base cavity needed to be effective. A cavity depth equal to the main-engine nozzle length showed a very small influence. The effectiveness of the cavity was pronounced when its depth was double that of the nozzles.

4) The surface of the cavity-producing side plates had considerable effect on its efficiency. A V-grooved surface was most effective in increasing base pressures.

5) Increased skin friction of the V-grooved surface canceled out its advantage of higher base-pressure increase over the smooth-surface cavity, and the two configurations resulted in similar reductions in the total drag of the Orbiter.

6) Because of the complex three-dimensional nature of the base flow, the trapped-vortex effect was effective only in the OMS pod region.

7) The cavity configuration maintained its effectiveness at all angles of attack. However, the effectiveness of the OMS pod fairing plate decreased with increasing angle of attack; the reduction in total drag due to it was almost negligible at AoA of 15 deg and higher.

8) Cavity ventilation/porosity was found to reduce the effectiveness of the cavity. Therefore, contrary to fully enclosed base cavities, a detrimental effect on base pressure for configurations where the cavity is not fully enclosed may be expected.

9) Combining the base cavity and OMS pods fairing plate resulted in a base-pressure increase of 25% and a total-drag reduction of 6.25%.

10) The advantage of a grooved surface cavity needs to be explored by determining the optimum groove geometry and methods to reduce its skin-friction contribution.

Acknowledgments

This work was supported by NASA Johnson Space Center under Contract NAS-18261 with R. E. Myerson and J. M. Caram as technical monitors.

References

[1]Meyerson, R. E., "An Experimental Study to Improve Space Shuttle Approach and Landing Characteristics," AIAA Paper 90-3075CP, Aug. 1990.

[2]Roshko, A., "On the Drag and Shedding Frequency of Two Dimensional Bluff Bodies," NACA TN 3169, July 1954.

[3]Kentfield, J. A. C., "Short Multi-step AfterBody Fairings," *Journal of Aircraft*, Vol. 21, No. 5, 1985, pp. 351–352.

[4]Mair, M. A., "The Effect of a Rear Mounted Disc on the Drag of a Blunt Based Body of Revolution," *The Aeronautical Quarterly*, Vol. XVI, Part 4, Nov. 1965, pp. 350–360.

[5]Nash, J. F., "A Discussion of 2D Turbulent Base Flows," Aeronautical Research Council, Reports & Memoranda 3468, Ministry of Technology, London, July 1967.

[6]Compton, W. B., "Effect on Base Drag of Recessing Bases of Conical Afterbodies at Subsonic and Transonic Speeds," NASA TN D-4821, 1968.

[7]Tanner, M., "Reduction of Base Drag," *Progress in Aerospace Sciences*, Vol. 16, No. 4, 1975, pp. 369–384.

[8]Tanner, M., "Base Cavity at Angle of Attack," *AIAA Journal*, Vol. 26, No. 3, 1988, pp. 376–377.

[9]Morel, T., "Effect of Base Cavities on the Aerodynamic Drag of an Axisymmetric Cylinder," *The Aeronautical Quarterly*, Vol. XXX, Part 2, May 1979, pp. 400–412.

[10]Friedberg, R. A., and Ahmed, A., "3-D Supersonic Combustion Experiments with Hydrogen in V-Troughs," AIAA Paper 82-0417, 1982.

[11]Viswanath, P. R., "Passive Devices for Axisymmetric Base Drag Reductions at Transonic Speeds," *Journal of Aircraft*, Vol. 25, No. 3, 1988, pp. 258–262.

[12]Viswanath, P. R., and Patil, S. R., "Effectiveness of Passive Devices for Axisymmetric Base Drag Reduction at Mach 2," *Journal of Spacecraft and Rockets*, Vol. 27, No. 3, 1990, pp. 234–237.

[13]Ahmed, A., Khan, M. J., and Varela-Rodriguez, E., "Base Drag Reduction of the Space Shuttle Orbiter," NASA CR-185671-0000, May 1992.

[14]Nichols, M. E., "Results of Investigations on 0.004 Scale Model 74-0 of the Configuration 4 (Modified) Space Shuttle Vehicle Orbiter in the NASA/MSFC 14-by-14-Inch Trisonic Wind Tunnel (OA131)," DMS-DR-2232, NASA-CR-141,521, March 1975.